J Bioenerg Biomembr (2010) 42:173–180
DOI 10.1007/s10863-010-9273-z

Unimolecular study of the interaction between the outer membrane protein OmpF from E. coli and an analogue of the HP(2–20) antimicrobial peptide

Aurelia Apetrei · Alina Asandei · Yoonkyung Park · Kyung-Soo Hahm · Mathias Winterhalter · Tudor Luchian

Received: 5 November 2009 / Accepted: 3 February 2010 / Published online: 24 February 2010

Abstract Little is known on antimicrobial peptide permeation through outer membrane channels in Gram-negative bacteria. Herein, we probed at a single-molecule level the interaction of two different peptides, magainin 2 and HPA3P with OmpF from E. coli. HPA3P is an analogue of the antimicrobial peptide HP(2–20) isolated from the N-terminal region of the Helicobacter pylori ribosomal protein. Our data show that the shorter and more charged HPA3P peptide is more accessible to the inner volume of the OmpF than magainin 2. We demonstrate the ability of HPA3P peptides to interact with OmpF in a voltage- and concentration-dependent manner, which does not rule out a novel mechanism by which such peptides could reach the periplasmic space of Gram-negative bacteria. Unexpectedly, we found that increasing the applied voltage led to an increase of the residence time of HPA3P peptide inside the pore, possibly reflecting electric field-induced changes in pore and peptide geometry.

Keywords Electrophysiology · Lipid membranes · OmpF porin · Antimicrobial peptides · Single-molecule recordings

A. Apetrei · A. Asandei · T. Luchian (✉)
Faculty of Physics, Laboratory of Biophysics and Medical Physics, Alexandru I. Cuza' University, Blvd. Carol I, No. 11, Iasi 700506, Romania
e-mail: luchian@uaic.ro

Y. Park · K.-S. Hahm
Research Center for Proteineous Materials, Chosun University, Gwangju, South Korea

M. Winterhalter
School of Engineering and Science, Jacobs University, Bremen, Germany

Introduction

Antimicrobial peptides (AMPs) are effector molecules of innate immunity and are synthesized by living organisms for the purpose of killing of Gram-positive and Gram-negative bacteria, fungi, parasites, enveloped viruses, and tumor cells (Zasloff 2002; Tossi 2005). They have attracted interest as a potential new class of antibiotics, or as a substitute or addition to conventional antibiotics to which many pathogens have acquired resistance (Hancock and Lehrer 1998; Brown and Hancock 2006; McPhee and Hancock 2005).

Most AMPs are cationic peptides composed of 12–50 amino acids and despite their wide heterogeneity in sequence and structure, antimicrobial peptides share several common features, such as a net positive charge of about +4 to +6, approximately 50–70% hydrophobic amino acids, and a potential to form an amphipathic α-helical structure in the presence of lipid membranes (Giangaspero et al. 2001;Yang et al. 2001). Many antimicrobial peptides are thought to exert their toxicity by permeabilizing the lipid matrix of cell membranes leading to leakage of ions and metabolites which in turn causes depolarization, loss of membrane-coupled respiration, and eventually cell death. To date, several molecular models have been proposed to answer how AMPs induce membrane permeabilization: among the most popular are the so-called 'barrel-stave', 'toroidal pore' and the 'carpet' models (Yang et al. 2001; Epand and Vogel 1999; Zelezetsky et al. 2005).

Antimicrobial peptide selectivity for prokaryotic cells relies largely on non-receptor mediated effects, driven by the recognition of physico-chemical properties of the cell membrane (Wade et al. 1990; Bessalle et al. 1990; Merrifield et al. 1995). Previous data revealed microbial killing at

concentrations below the lytic activity indicating the possibility some antimicrobial peptides interact with intracellular targets, inducing cell damage by some other mechanism like inhibition of the cell-wall synthesis, nucleic acids, protein or enzymatic activity (Oren and Shai 1996; Park et al. 1998; Subbalakshmi and Sitaram 1998; Kragol et al. 2001; Lehrer et al. 1989; Shimoda et al. 1995; Chan et al. 1998). However, how these peptides permeate the inner membrane is unknown. Obviously in a first step the peptides must cross the outer membrane and likely porins as water filled membrane channels are possible pathways (Bredin et al. 2003; Nikaido 2003). One of the most abundant porin in E. coli is OmpF (>10^5 copies per cell) (Danelon et al. 2003; Schirmer 1998). A molecular model of one monomer from the OmpF trimeric protein is shown in Fig. 1 (PDB entry 2 omf). The general architecture consists of a rather large hollow β-barrel structure, formed by antiparallel arrangement of 16 β-strands. These strands are connected by short loops or regular turns on the periplasmic side and by long irregular loops situated on the extracellular side, and three such barrels form stable trimeric molecules that can be dissociated only upon denaturation.

One of the eight extracellular loops (L3) of such porins folds back into the pore lumen; about half way down the channel, an aspartate (D113) and glutamate (E117) from the tip of L3 face three arginine groups located at the channel wall (R42, R82 and R132), creating an asymmetrically shaped constriction zone of about 0.7×1.1 nm^2 in area which could allow for the threading of an unfolded polypeptide (Sharma and Cramer 2007).

Notably, it is known that several outer membrane proteins play important roles as receptors for phage and colicins (Cascales et al. 2007). For example, the 551 residue rRNase colicin E3 interacts tightly with the BtuB receptor and exerts its cytotoxic effect through the endoribonucleolytic action of its 96 residue C-terminal domain, which is transported into the cytoplasm and uses its N-terminal translocation domain to interact with OmpF, its putative receptor-translocator (Housden et al. 2005; Law et al. 2003; Kurisu et al. 2003; Zakharov et al. 2004).

Recently, we investigated the mechanism of action of the HPA3 peptide, an analogue of the linear antimicrobial peptide, HP(2–20), isolated from the N-terminal region of the Helicobacter pylori ribosomal protein (Mereuta et al. 2009; Mereuta et al. 2008; Lee et al. 2006). The HP(2-20) peptide was shown to display several important functional characteristics, such as: bactericidal, neutrophil chemoattractant, and it activates phagocyte NADPH oxidase to produce reactive oxygen species. Moreover, HP(2–20) and its analogues specifically recognize common immune elicitors, including chitin, peptidoglycan, and LPS, thus becoming very promising candidates for the development of new peptide-based antibiotic agents (Park et al. 2008).

The interaction of peptides with protein pores is of paramount relevance in biology, and protein translocation in the endoplasmic reticulum, from the cytoplasm into mitochondria or across the chloroplast membrane constitute only few selected examples (Hinnah et al. 2002). Previous works have examined the partitioning of synthetic peptides into α-hemolysin, another β-barrel protein pore (Movileanu et al. 2005; Sutherland et al. 2004 ; Stefureac et al. 2006; Wolfe et al. 2007).

Nevertheless, scarce data exists regarding antimicrobial peptides interaction with transmembrane proteins with roles in molecular transport across bacterial membranes. Herein we probed at single-molecule level the exchange between the aqueous phase and the β-barrel of the OmpF protein of magainin 2 and HPA3P, an analogue of the antimicrobial peptide HP(2–20), known to be good scaffolds for engineering novel antibiotic agents (Park et al. 2008).

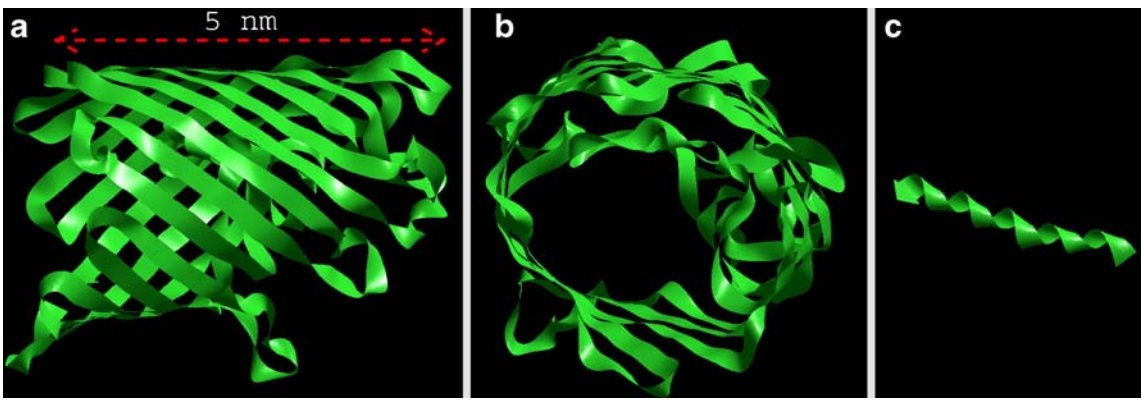

Fig. 1 (**a**) Side and (**b**) top view of a single OmpF monomer. Drawn to the scale, in panel (**c**) it is shown the non-minimized appearance of the HPA3P peptide, constrained to an α-helix (note that in water the peptide most likely assumes a random-coil like tertiary structure). Images were prepared in RasTop 2.2

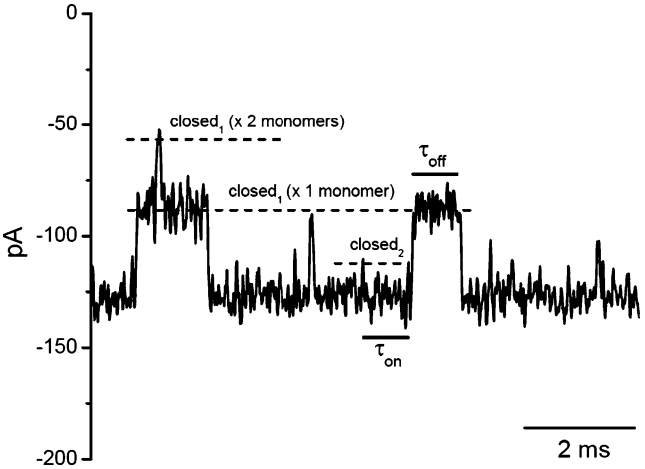

Fig. 2 Ion current trace showing the main features of cis-added, HPA3P-induced fluctuations measured at −90 mV through a single OmpF trimer, seen here as upwards step-like alterations of the ion current through the protein (see text)

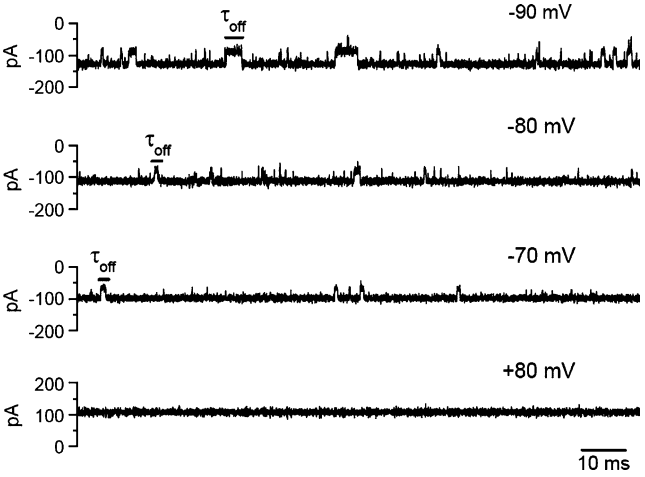

Fig. 4 Typical ion current trace showing at the single-molecule level the voltage-dependent reversible block of OmpF by HPA3P (10 μM), as seen in electrical recordings

Experimental section

Single molecule electrophysiology

Planar bilayer membranes were obtained as previously described from 1,2-diphytanoyl-sn-glycerophosphocholine (Avanti Polar Lipids, Alabaster, AL) (Chiriac and Luchian 2007; Asandei et al. 2008). The electrolyte from both the cis and trans sides of the bilayer chamber contained 0.5 M NaCl, 5 mM MES (Sigma-Aldrich), and pH was set to 6.2 to minimize stepwise current transients observed as a result of reversible protonation of ionizable residues located on the constriction zone (Nestorovich et al. 2003). Measurements were performed at room temperature (26°C±1°C). Single channel insertion of the OmpF protein was achieved by adding ~1 μl from a dilute stock solution made in 0.5 M NaCl and 1% (v/v) of octyl POE to the grounded, cis chamber. Currents were amplified with either a resistive (EPC8, HEKA, Germany) or a capacitive headstage patch-clamp amplifier (Axopatch 200B, Molecular Devices, USA). Amplified signals were low-pass filtered at 10 kHz, and data acquisition was performed with a NI PCI 6221, 16-bit acquisition board (National Instruments, USA) at a sampling frequency of 100 kHz, within LabVIEW 8.20. Unless stated otherwise, magainin 2 (GIGKFLHSAKKFGKAFVGEIMNS, ≥97% HPLC, Sigma-Aldrich) and HPA3P (AKKVFKRLPKLFSKIWNWK) were

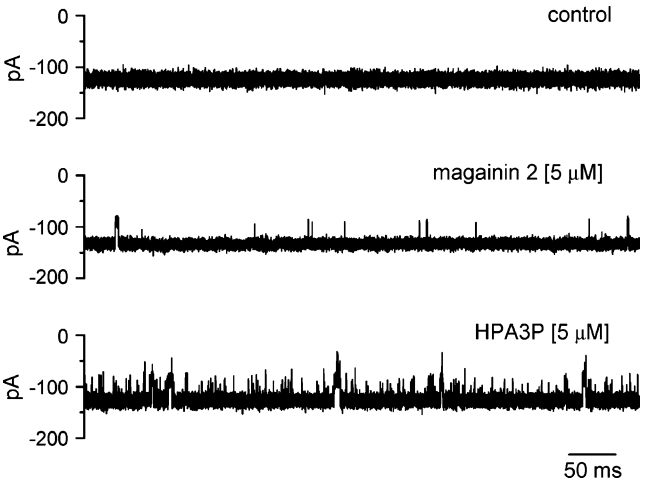

Fig. 3 Typical ion current trace measured at −90 mV through a single OmpF channel, in absence of added peptide (control) and in presence (cis side addition) of either magainin 2 or HPA3P antimicrobial peptides. In the upper (control) trace the current is silent with negligible fluctuations. In presence of HPA3P peptide one of the three monomer OmpF pores gets spontaneously blocked by an incoming peptide and this leads to reversible alterations of the single-molecule current recorded

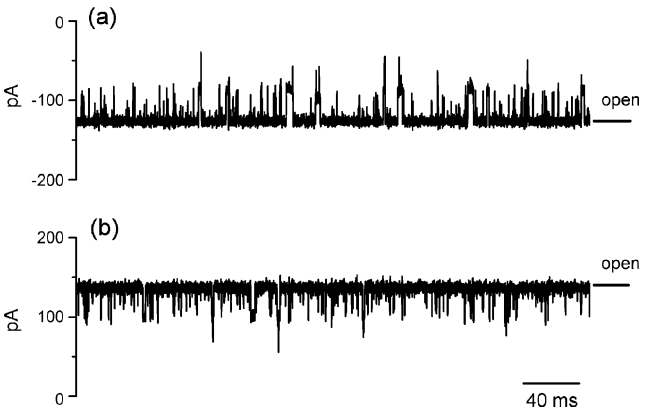

Fig. 5 Typical traces of ion currents through a single OmpF channel inserted into planar lipid membranes, in the presence of the 10 μM HPA3P added on the cis side (trace 'a'; −90 mV) or the trans side (trace 'b'; + 90 mV) of the membrane. The fully open state of a single trimeric OmpF channel is indicated by dash

added on the cis side of the membrane from stock solutions made in distilled water. The particular lipids chosen in this study to construct planar membranes ensured virtually absent insertion of cationic magainin 2 and HPA3P peptides under working conditions used throughout.

Peptide synthesis and purification

HPA3P was synthesized via solid-phase methods with Fmoc (N-(9-fluorenyl)methoxycarbonyl)-protected amino acids on a CEM microwave peptide synthesizer. 4-Methyl benzhydrylamine resin (Novabiochem) (0.55 mmol/g) was employed to create the amidated C-terminus. For each coupling step, the Fmoc-protected amino acid and coupling reagents were added in a 10-fold molar excess with regard to resin concentration. Coupling (60–90 min) was conducted with DCC (dicyclohexylcarbodiimide) and HOBT (1-hydroxy benzotriazole) in NMP (N-methyl-2-pyrrolidone). Cleavage from the resin and the deprotection of the synthesized peptide were conducted using a solution of 90% trifluoroacetic acid, 3% water, 1% triisopropylsilane and 2% each of 1,2-ethanedithiol, thioanisole, and phenol. After repeated ether precipitation, the crude peptide was purified via reversed-phase preparative HPLC on a Waters 15-μm Deltapak C18 column (19×300 mm) using an appropriate 0–60% acetonitrile gradient in 0.1% trifluoroacetic acid. The purity of the purified peptide was then determined via analytical reversed-phase HPLC using a Vydac C18 column (4.6×250 mm, 300 Å, 5 nm). The molecular masses of the peptides were verified with a matrix-assisted laser desorption ionization mass spectrometer (MALDI II, Kratos Analytical Ins.).

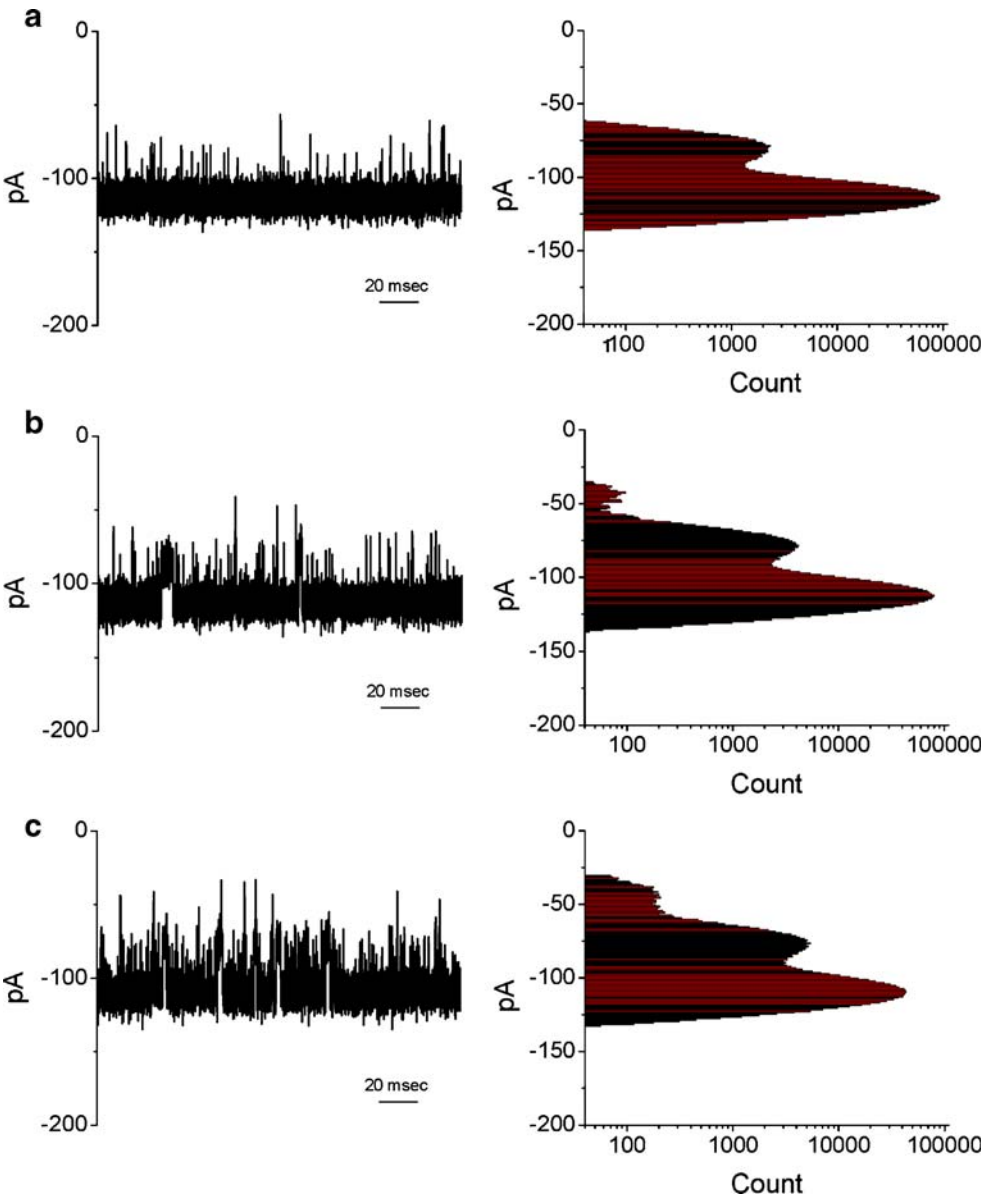

Fig. 6 Representative traces showing ion currents fluctuations through single OmpF protein reconstituted into planar lipid membranes measured at −80 mV, in the presence of cis-added (**a**) 5 μM (**b**) 10 μM and (**c**) 30 μM HPA3P. On the right-had side the corresponding amplitude histogram is given

Statistical analysis of single-molecule data

Statistical analysis of peptide-induced fluctuations was done as previously published for small molecule permeation (Nestorovich et al. 2002). In Fig. 2 we show typical events after peptide addition. We used a simplified model accounting for the interaction of peptide with the lumen of the OmpF monomer which gives rise to transitions from the fully open trimer ('open') to the complete blockage of one of the monomers in the channel trimer ('closed$_1$'). The additional events stemming from partially-blocked monomers which may occur via simple collisions of the peptides with the porin ('closed$_2$'), whereby peptides fail to further diffuse across the porin, were neglected during dwell-time analysis and further determination of the kinetic constants. In rare cases blocking of two channels has been observed. As previously suggested (Movileanu et al. 2005; Sutherland et al. 2004) we interpret the blocking event as peptide penetration into the channel lumen, giving rise to 'closed$_1$'-like events.

Due to a such heterogeneity with regard to various types of interaction events between the porin and peptides, and unlike other specific cases when such events are seen relatively clear, in our case we tried to avoid spectral analysis or automatic selection of blocking events which would have automatically accounted for type '2' events as well and introduce errors in our kinetic evaluations. Instead, we resorted to the 'hand-picking' of all events for further analysis. Therefore, all subsequent statistical data analysis was made as we previously described (Luchian et al. 2003), i.e. without involving histograms but averages of time interval events instead. However, as theory demonstrates (Colquhoun 1971), kinetic data inferred from either histogram analysis or average on time events are equivalent. We associate the number of full blockage events with an on-rate (k_{on}) which was inferred from the reciprocal of the mean inter-event interval (τ_{on}) separating the fully open trimer from the complete blockage of one of the monomers (i.e., the 'closed$_1$' state). Quantitative evaluation of reaction rates was based on at least three independent experiments, and values were expressed as mean values ± S.E.M.

Results and discussion

After formation of a stable lipid bilayer, we inserted a single trimeric OmpF pore which was observed by a sudden jump in the ion current (Asandei et al. 2008). Addition of micromolar concentrations of either magainin 2 or HPA3P peptides to the cis side of the bilayer produces reversible channel blockades of OmpF. The shorter, more charged HPA3P peptide proved to be more accessible to the inner volume of the OmpF compared to magainin 2 (Fig. 3). The HPA3P peptide interacts readily with the constriction region of the OmpF channel leading to long-lived, fully blocking events of individual monomers, and renders the peptide translocation events visible. Due to the increased ability of HPA3P vs. magainin 2 to penetrate the channel we focus in the following on this peptide.

It is important to note that HPA3P peptide addition to the cis side of the membrane required trans-negative potentials to promote the interaction between a peptide and an OmpF protein, whereas no binding events are seen with the orientation of the electric field reversed (i.e., positive potentials on the trans side) (Fig. 4). Apparently, due to their cationic charge, the presence of positive potentials on the trans side makes it unlikely for HPA3P peptides to overcome via thermal diffusion the electrical barrier encountered in their way towards and inside the pore. An immediate interpretation of such data is that HPA3P peptides are driven electrophoretically through the pore and a properly oriented electric field across the porin is required to drive the positively charged peptide into the pore, thus plugging it.

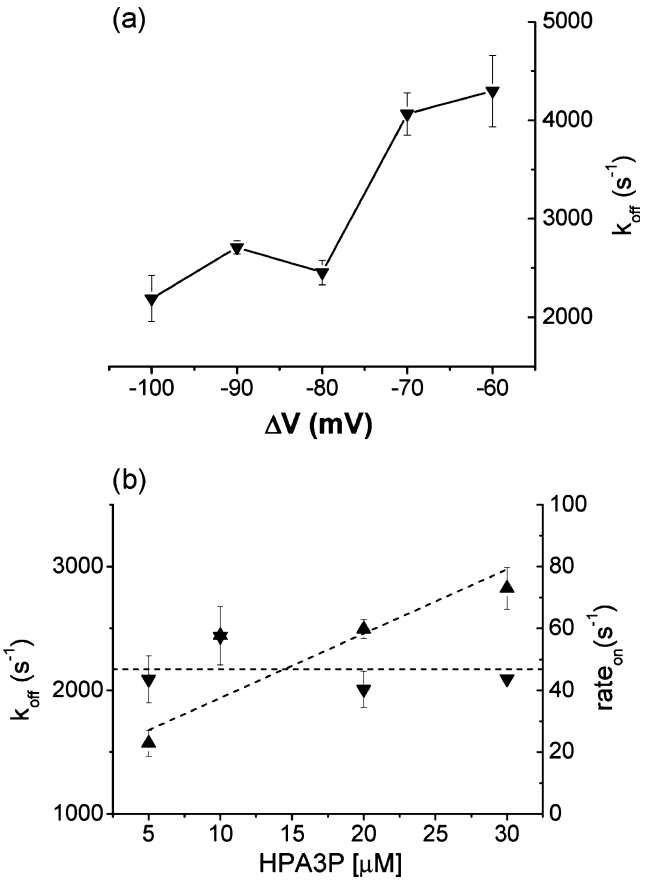

Fig. 7 (**a**) Voltage-dependence of the dissociation rate (k_{off}; *black down-pointing triangle*) of HPA3P measured at a 10 μM and (b) the concentration-dependence of the association ($rate_{on}$; *black up-pointing triangle*) and dissociation rates (k_{off}; *black down-pointing triangle*) measured at −80 mV

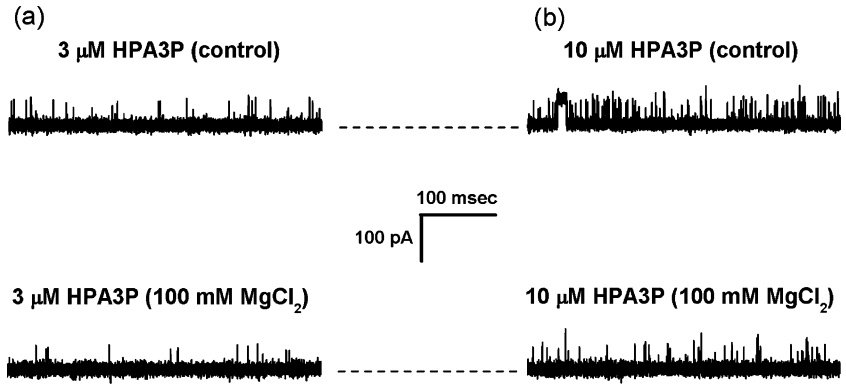

Fig. 8 Selected traces showing the inhibitory effect of both side addition of 100 mM $MgCl_2$ on the blocking events of cis-added HPA3P peptide at 3 μM (panel a) and 10 μM (panel b) and at −100 mV transmembrane voltage. The fully open state of a single trimeric OmpF channel in both panels is marked with a dashed line. The upward fluctuations correspond to peptide blocking

A surprising observation is that increasing the applied voltage leads to an increase of the residence time (τ_{off}) of HPA3P in the construction zone (Fig. 4). Although this is somewhat contradictory, it might be caused by conformational changes in the constriction zone of OmpF under strong electric fields. Similarly, it is interesting to note that previous work on DNA translocation revealed that increasing the applied voltage increased the duration of the DNA-current blockades in small artificial silicon nitride nanopores (diameters of ~1 nm) (Li et al. 2003; Heng et al. 2004). The latter authors proposed that the rate-limiting step for the DNA translocation is not the passage of DNA through the pore only, but the search for an optimal conformation that facilitates the translocation (Aksimentiev et al. 2004).

Interestingly, when peptide was added to the trans side of the OmpF, positively applied potentials were needed to generate blocking events. In Fig. 5 we display both. Visual inspection of such traces reveals that the peptide is able to enter and reversibly block the channel from both extracellular and intracellular openings. Detailed statistical analysis of time intervals associated to full blocking events of one monomer by the trans-added HPA3P peptide (denoted above by 'closed$_1$') showed that +90 mV transmembrane voltage caused an $k_{off;\ trans;\ +90\ mV}$=3453±310 s^{-1}, similar to that obtained when the peptide was added on the cis side and the voltage bias was set to −90 mV ($k_{off;\ cis;\ -90\ mV}$= 2709±133 s^{-1}). Based on this and like in previous publications (Kullman et al. 2002), we do not completely rule out that full HPA3P-induced blocking events may reflect peptide translocation.

In a further experiment we investigated the concentration dependence of the HPA3P interaction with OmpF, which is shown in Fig. 6. It is seen that larger aqueous concentrations of the HPA3P peptide lead to an increase in the number of peptide-induced blocking events, and this can be visually quantified by a close inspection of the amplitude histogram of such events (Fig. 6).

In Fig. 7 we show the linear dependence of the number of the fully blocking events. As previously shown for sugar or antibiotic translocation, the HPA3P - OmpF interaction could be related to a symmetric two barrier-one affinity site model (Kullman et al. 2002; Nestorovich et al. 2002). In our case the peptide concentration is far to reach the channel saturation. In this case, assuming the three OmpF monomers to be uncorrelated, the association rate of the peptide to any of the monomers from the trimeric OmpF ($rate_{on}$) is inversely proportional to the inter-events dwell time separating the fully open trimer from the complete blockage of one of the monomers divided by three, whereas the dissociation rate (off-rate, k_{off}) is inversely related to the residence (dwell) time (Danelon et al. 2003; Kullman et al. 2002; Nestorovich et al. 2002).

Plots of the association ($rate_{on}$;▲) and dissociation rates (k_{off};▼) measured at −80 mV versus the concentration of HPA3P are suggestive of a simple bimolecular interaction

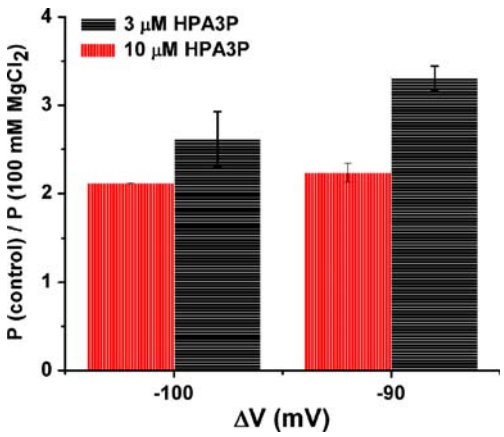

Fig. 9 Quantitative description of the extent to which the presence of cis- and trans-added 100 mM $MgCl_2$ modulates the extent of occurring HPA3P-induced binding events, as measured at −100 and −90 mV

(Fig. 7). The rate constant of peptide association to single monomers from the trimeric OmpF, k_{on}, was derived from the slope of the plot of $rate_{on}$ vs. aqueous concentration of HPA3P (k_{on}=2.1±0.5 μM^{-1} s^{-1}), and by virtue of the simple bimolecular model taken into account, $rate_{off}$ equals the dissociation constant k_{off} (k_{off}=2170±5 s^{-1}). A further test of peptide interaction is to probe a possible competitive interaction with high Mg^{2+} concentration. In a recent crystallographic study on the interactions of the OmpF with the unfolded N-terminal domain (T83) of colicin E3, a binding site for Mg^{2+} inside the channel was observed (Yamashita et al. 2008). We expect that in presence of Mg^{2+} the interaction of the peptide would be reduced.

As shown in Fig. 8, panel a, our single-molecule recordings indicate that Mg^{2+} added symmetrically at a concentration of 100 mM, reduced significantly the peptide interaction with OmpF. We reasoned that if a competition exists between Mg^{2+} and the peptide for their binding to the selectivity filter of the porin instead of a simple screening effect induced by $MgCl_2$, the Mg^{2+} - induced decrease in the peptide-mediated binding events would diminish in conditions whereby the concentration of the peptide increases and Mg^{2+} concentrations remains unchanged. The ratio of the probability of the peptide-induced complete blockage of one of the monomers in the channel trimer (assigned to the '$closed_1$' state) in the absence (control) and presence of 100 mM $MgCl_2$ is seen to decrease once HPA3P concentration triples, indicating a competitive binding mechanism of Mg^{2+} ions and peptide to the constriction region of one OmpF monomer (Fig. 9).

This in turn led us to believe that the complete blockage, peptide-induced binding events seen in our recordings may reflect their reversible interactions with the selectivity filter of the porin, which helps capture and possibly translocate peptides entering the channel. In up-coming experiments we plan to further study this putative competitive binding mechanism of Mg^{2+} ions and peptide to the constriction region of one OmpF monomer by employing a wider range of peptide concentrations. Interestingly, it is apparent that the holding potential alters the competitive binding of Mg^{2+} ions and peptides to the constriction region of one OmpF monomer, as higher values of the holding potential are seen to reduce the access of Mg^{2+} ions binding to the constriction region of the porin, and further enlightenment of this effect will constitute a target of up-coming experiments.

Conclusion

Single-molecule experiments have revealed that addition of micromolar concentrations from either magainin 2 or HPA3P peptides produces reversible OmpF blockades in a voltage- and concentration-dependent manner. Our data do not exclude a novel paradigm that such peptides may reach the inner membrane of Gram-negative bacteria through OmpF under transmembrane voltage. An important question with respect to in-vivo relevance of antimicrobial peptides transport through porins is the magnitude of the electrostatic potential needed to drive the peptide across the channel. Due to the large amount of porins no significant potential drop can be maintained. However a Donnan potential could be postulated due to the large amount of charged polymers in the periplasmic space (Lindemann and Winterhalter 2006). Charged polymers, electrical charges associated with anionic lipids may generate surface and dipole potentials of rather elevated magnitude in the outer membrane, that give rise to a potential difference between the inner and outer monolayers of the outer membrane of 40–80 mV, negative on the periplasmic side of the outer membrane (Zakharov et al. 2004; Seydel et al. 1992; Wiese et al. 1996 ; Arzo et al. 2006). Consequently, such a potential gradient could constitute a possible driving force for cationic macromolecules diffusion through OmpF porins. Future work involving specifically engineered peptides (e.g., various charge, length, hydrophobicity) will help us pinpoint physical factors that determine and thus optimize selectivity features of the OmpF porin towards aqueous peptides with antimicrobial characteristics, under various physical circumstances.

Acknowledgments We acknowledge the support offered by the Romanian Ministry of Research and Technology through grants PN-2 61-16 (2007) (T. Luchian) and PN-2 62-061 (2008) (T. Luchian). The financial support offered by the 'Alexandru I. Cuza' University (A. Apetrei) is greatly acknowledged. We thank Professor Hagan Bayley (University of Oxford) for stimulating discussions on an early stage of this work. Suggestions made by referees toward improving the interpretation of some of our data are also acknowledged.

References

Aksimentiev A, Heng JB, Timp G, Schulten K (2004) Biophys J 87:2086–2097

Arzo MA, Celma JJG, Cervera J, Alcaraz A, Aguilella VM (2006) Bioelectrochemistry 71:22–29

Asandei A, Mereuta L, Luchian T (2008) Biophy Chem 135:32–40

Bessalle R, Kapitkovsky A, Gorea A, Shalit I, Fridkin M (1990) FEBS Lett 274:151–155

Bredin J, Simonet V, Iyer R, Delcour AH, Pages JM (2003) Biochem J 376:245–252

Brown KL, Hancock RE (2006) Curr Opin Immunol 18:24–30

Cascales E, Buchanan SK, Duche D, Kleanthous C, Lloubes R, Postle K, Riley M, Slatin S, Cavard D (2007) Microbiol Mol Biol Rev 71:158–229

Chan SC, Yau WL, Wang W, Smith DK, Sheu F-S, Chen HM (1998) J Pept Sci 4:413–425

Chiriac R, Luchian T (2007) Biophy Chem 130:139–147

Colquhoun D (1971) Lectures on biostatistics: an introduction to statistics with applications in biology and medicine. Clarendon, Oxford

Danelon C, Suenaga A, Winterhalter M, Yamato I (2003) Biophys Chem 104:591–603
Epand RM, Vogel HJ (1999) Biochim Biophys Acta 1462:11–28
Giangaspero A, Sandri L, Tossi A (2001) Eur J Biochem 268:5589–5600
Hancock REW, Lehrer R (1998) Trends Biotechnol 16:82–88
Heng JB, Ho C, Kim T, Timp R, Aksimentiev A, Grinkova YV, Sligar S, Schulten K, Timp G (2004) Biophys J 87:2905–2911
Hinnah SC, Wagner R, Sveshnikova N, Harrer R, Soll J (2002) Biophys J 83:899–911
Housden NG, Loftus SR, Moore GR, James R, Kleanthous C (2005) Proc. Natl Acad Sci USA 102:13849–13854
Kragol G, Lovas S, Varadi G, Condie BA, Hoffmann R, Otvos L Jr (2001) Biochemistry 40:3016–3026
Kullman L, Winterhalter M, Bezrukov SM (2002) Biophys J 82:803–812
Kurisu G, Zakharov SD, Zhalnina MV, Bano S, Eroukova VY, Rokitskaya TI, Antonenko YN, Wiener MC, Cramer WA (2003) Nat Struct Biol 10:948–954
Law CJ, Penfold CN, Walker DC, Moore GR, James R, Kleanthous C (2003) FEBS Lett 545:127–132
Lee KH, Lee DG, Park Y, Kang D-I, Shin SY, Hahm K-S, Kim Y (2006) Biochem J 394:105–114
Lehrer RI, Barton A, Daher KA, Harwig SSL, Ganz T, Selsted ME (1989) J Clin Invest 84:553–561
Li J, Gersho M, Stein D, Brandin E, Aziz MJ, Golovchenko JA (2003) Nat Mater 2:611–615
Lindemann M, Winterhalter M (2006) IEE Proc Nanobiotechnol 153:107–111
Luchian T, Shin S-H, Bayley H (2003) Angew Chem Int Ed 42:1925–1929
McPhee JB, Hancock RE (2005) J Pept Sci 11:677–687
Mereuta L, Luchian T, Park Y, Hahm K-S (2008) Biochem Biophys Res Commun 373:467–472
Mereuta L, Luchian T, Park Y, Hahm K-S (2009) J Bioenerg Biomem 41:79–84
Merrifield RB, Juvvadi P, Andreu D, Ubach J, Boman A, Boman HG (1995) Proc Natl Acad Sci U S A 92:3449–3453
Movileanu L, Schmittschmitt JP, Scholtz JM, Bayley H (2005) Biophys J 89:1030–1045
Nestorovich EM, Danelon C, Winterhalter M, Bezrukov SM (2002) Proc. Natl Acad Sci USA 99(15):9789–9794
Nestorovich EM, Rostovtseva TK, Bezrukov SM (2003) Biophys J 85:1–12
Nikaido H (2003) Microbiol Mol Biol Rev 67:593–656
Oren Z, Shai Y (1996) Eur J Biochem 237:303–310
Park CB, Kim HS, Kim SC (1998) Biochem Biophys Res Commun 244:253–257
Park SC, Kim MH, Hossain MA, Shin SY, Kim Y, Stella L, Wade JD, Park Y, Hahm K-S (2008) Biochim Biophys Acta 1788:229–241
Seydel U, Eberstein W, Schroder G, Brandenburg KZ (1992) Naturforsch 47c:757–761
Schirmer T (1998) J Struct Biol 121:101–109
Sharma O, Cramer WA (2007) J Bacteriol 189:363–368
Shimoda M, Ohki K, Shimamoto Y, Kohashi O (1995) Infect Immun 63:2886–2891
Stefureac R, Long Y-T, Kraatz HB, Howard P, Lee JS (2006) Biochemistry 45:9172–9179
Subbalakshmi C, Sitaram N (1998) FEMS Microbiol Lett 160:91–96
Sutherland TC, Long Y-T, Stefureac RI, Bediako-Amoa I, Kraatz HB, Lee JS (2004) Nanoletters 4:1273–1277
Tossi A (2005) Curr Protein Pept Sci 6:1–3
Wade D, Boman A, Wahlin B, Drain CM, Andreu D, Boman HG, Merrifield RB (1990) Proc Natl Acad Sci U S A 87:4761–4765
Wiese A, Reiner JO, Brandenburg K, Kawahara K, Zahringer U, Seydel U (1996) Biophys J 70:321–329
Wolfe AJ, Mohammad MM, Cheley S, Bayley H, Movileanu L (2007) J Am Chem Soc 129:14034–14041
Yamashita E, Zhalnina MV, Zakharov SD, Sharma O, Cramer WA (2008) EMBO J 27:2171–2180
Yang L, Harroun TA, Weiss TM, Ding L, Huang HW (2001) Biophys J 81:1475–1485
Zakharov SD, Eroukova VY, Rokitskaya TI, Zhalnina MV, Sharma O, Loll PJ, Zgurskaya HI, Antonenko YN, Cramer WA (2004) Biophys J 87:3901–3911
Zasloff M (2002) Nature 415:389–395
Zelezetsky I, Pacor S, Pag U, Papo N, Shai Y, Sahl HG, Tossi A (2005) Biochem J 390:177–188